

# Oxidation states and ionicity

Aron Walsh<sup>1,2</sup>, Alexey A. Sokol<sup>3</sup>, John Buckeridge<sup>3</sup>, David O. Scanlon<sup>3,4</sup>, and  
C. Richard A. Catlow<sup>3,5</sup>

<sup>1</sup>Department of Materials, Imperial College London, London SW7 2AZ, UK

<sup>2</sup>Department of Materials Science and Engineering, Yonsei University, Seoul 03722, Korea

<sup>3</sup>Department of Chemistry and Thomas Young Centre, University College London, London WC1H 0AJ, UK

<sup>4</sup>Diamond Light Source Ltd., Harwell Science and Innovation Campus, Oxfordshire OX11 0DE, UK

<sup>5</sup>School of Chemistry, Cardiff University, Cardiff CF10 3AT, UK

**The concepts of oxidation state and atomic charge are entangled in modern materials science. We distinguish between these quantities and consider their fundamental limitations and utility for understanding material properties. We discuss the nature of bonding between atoms and the techniques that have been developed for partitioning electron density. Whilst formal oxidation states help us count electrons (in ions, bonds, lone pairs, etc.), variously defined atomic charges are usefully employed in the description of physical processes including dielectric response and electronic spectroscopies. Such partial charges are introduced as quantitative measures in simple mechanistic models of a more complex reality, and therefore may not be comparable or transferable. In contrast, oxidation states are defined to be universal, with deviations constituting exciting challenges as evidenced in mixed-valence compounds, electrified, and highly-correlated systems. This Perspective covers how these concepts have evolved in recent years, our current understanding, and their significance.**

The concept of *oxydationsstufe* was developed over two centuries ago to describe the observed reactions of elements with oxygen<sup>1</sup>. Such chemical reactions are quantised, with distinct changes in structure and properties as more oxygen is bound by an element (e.g.  $6\text{Fe} + 3\text{O}_2 \rightarrow 6\text{FeO} + \text{O}_2 \rightarrow 2\text{Fe}_3\text{O}_4 + \frac{1}{2}\text{O}_2 \rightarrow 3\text{Fe}_2\text{O}_3$ ). The modern oxidation state is defined as “the degree of oxidation of an atom in terms of counting electrons”, where the nominal counting of electrons is performed following an agreed-upon set of rules<sup>2</sup>.

This Perspective focusses on chemical bonding in solids, where discussion almost invariably makes reference to oxidation states, ionicities, covalency, and charge distributions, which are indeed powerful concepts across the chemical sciences. Despite their widespread use, however, there are uncertainties and ambiguities about the concepts and their interrelationships. The debate became so heated in the 1960s that there was a sequence of three publications in *Nature* on this topic arguing different perspectives: Goodman discussed the role of atomic electronegativity in the distribution of electrons in solids<sup>3</sup>; Mooser and Pearson emphasised that bond ionicity is a theoretical concept that depends on the approximation employed<sup>4</sup>; while Cochran focused on what can and cannot be measured in practice<sup>5</sup>.

As argued previously, the concept of ionicity in solids remains intrinsically ambiguous<sup>6</sup>: charge distributions can be calculated and measured with growing accuracy, but there are several different plausible schemes for their partition between the component atoms. Alternative definitions and measures of ionicity are necessary to describe other properties, for example dielectric response, which depend on charge distribution. Further difficulties arise when the equilibrium charge distribution is linked to oxidation state. We may agree

47 that a molecule or solid has a metal in its highest accessible oxidation state, but experiment  
48 and theory will often reveal significant electron density in its valence shell orbitals.

49 Debate continues on the topic and is indeed very much alive<sup>7-10</sup>. We attempt to address  
50 these problems and to show how ionicity, charge distribution, and oxidation state  
51 interrelate and can be meaningfully used. We further discuss cases where genuine  
52 ambiguities and challenges exist for mixed-valence compounds, as well as new generations  
53 of quantum materials at the frontier of materials science.

#### 54 Utility of Formal Oxidation States

55 Electron counting is at the heart of our understanding of, and approach to, chemical  
56 bonding<sup>11</sup>. In one trivial example, two hydrogen atoms (one-electron species) interact  
57 through a two-electron covalent bond formed by filled bonding and empty anti-bonding  
58 orbitals. In the solid state, a similar case would be crystalline silicon, where two-electron  
59 two-centre covalent bonds are formed between nearest-neighbour silicon atoms in a  
60 periodic structure. In both cases, effective charges are usually assumed to be zero. The  
61 valence number can however be defined as I (hydrogen) and IV (silicon), which represents  
62 the number of electrons involved in (or available for) chemical bonding.

63 The combination of a metal with a more electronegative element can be described by the  
64 formation of an ionic (or heteropolar) bond. One such case is LiF, where one-electron  
65 transfer from Li ( $1s^2 2s^1$ ) to F ( $2s^2 2p^5$ ) results in closed-shell  $Li^+$  ( $1s^2 2s^0$ ) and  $F^-$  ( $2s^2 2p^6$ )  
66 electronic configurations. While one can assign different effective charges to Li and F, the  
67 formation of a complete closed shell around F and the depletion of the valence charge  
68 density around Li are unambiguously detected by experiment and electronic structure  
69 calculations. Perhaps, the most important observation here is that the electron associated  
70 with Li and all of the originally five p electrons of F take part in the resulting valence shell of  
71 the compound. Following simple octet rules for forming a closed-shell (diamagnetic)  
72 compound, the outcome we described can trivially be predicted for more complex chemical  
73 compounds.

74 These examples of both covalent and ionic interactions can be conveniently described using  
75 formal oxidation states. The value of oxidation state for each atom in a solid can be assigned  
76 following a set of rules (see Box 1), e.g. the oxidation state of an atom in its elemental  
77 standard state is 0. A less trivial example is a multi-component solid such as the high-  
78 temperature superconductor  $YBa_2Cu_3O_7$ . Here, the oxidation state of O is -2, which means  
79 that the sum of oxidation states for  $Y + 2Ba + 3Cu = 14$  to provide the electrons involved in  
80 the bonding with oxygen. The common oxidation state of Y is +3, that of Ba is +2, so seven  
81 electrons need to be donated by three Cu atoms (assuming complete reduction of oxygen).  
82 The common oxidation states of Cu are +2 as in cupric oxide (CuO) and +1 in cuprous oxide  
83 ( $Cu_2O$ ). The unusual electron count in  $YBa_2Cu_3O_7$  requires either an additional electron  
84 (oxidation) from Cu to the +3 state or a hole stabilised on oxygen – often described as a  
85 polaron – which leads to its exotic condensed matter physics<sup>12</sup>. This conclusion is made in  
86 the absence of any substantial input from theory or experiment, but is crucial in  
87 understanding the properties of the material, and demonstrates the importance and power  
88 of these simple approaches.

89 While these concepts are easily transferable to the important area of mixed-anion  
90 compounds<sup>13</sup>, more involved consideration of the structure and bonding is required for the  
91 cases of polyion systems, where groups of atoms form sub-units that carry a formal charge.  
92 In BaSi, the usual oxidation states of Ba +2 and Si -4 fail to deliver a charge neutral

93 stoichiometric unit; however, the structure contains chains of covalent Si-Si bonds, where  
94 each Si adopts a -2 oxidation state. For  $\text{Ba}_3\text{Si}_4$ , discrete  $\text{Si}_4^{6-}$  polyanions are formed with  
95 internal Si-Si bonds, which ensures charge neutrality when combined with three Ba +2  
96 cations. There have been recent applications of such Zintl compounds in the field of  
97 thermoelectrics<sup>14,15</sup>.

98 Beyond predicting the outcomes of chemical reactions and the stoichiometry of compounds,  
99 oxidation states also have a utility in the description of physical properties. Oxidation states  
100 underpin a number of successful heuristic tools in molecular and solid-state chemistry,  
101 including the valence-shell electron-pair repulsion (VSEPR) theory for predicting structure<sup>16</sup>,  
102 and ligand and crystal field theory for predicting structure and spectroscopic response, in  
103 particular of transitional metal complexes and materials<sup>17</sup>. One example is Mn, of which  
104 there are seven positive oxidation states, where Mn(VII) corresponds to the removal of all of  
105 the valence electrons and formal configuration of  $3d^0$ . In the solid state, MnO corresponds  
106 Mn(II) ( $3d^5$ ), where the high spin state of  $5/2\hbar$  is observed, while  $\text{MnO}_2$  contains Mn(IV)  
107 ( $3d^3$ ), with a corresponding high spin state of  $3/2\hbar$ . The intermediate case of  $\text{Mn}_2\text{O}_3$  contains  
108 Mn(III) ( $3d^4$ ), which is Jahn-Teller active and results in a frustrated magnetic interactions in  
109 its ground state bixbyite crystal structure<sup>18</sup>. Each of these oxidation states of Mn can be  
110 easily distinguished from their distinct spectroscopic and magnetic signatures<sup>19</sup>.

111 Assigning formal oxidation states allows us to understand and rationalise key properties of  
112 the materials, but it is not a statement about effective charge: assigning an oxidation state  
113 of +7 to Mn in, for example, the compound  $\text{KMnO}_4$  does not imply, as argued above, that a  
114 calculated or experimentally measured charge density analysis will find zero charge density  
115 in the 3d orbitals; but it does indicate that all the 3d electrons are directly involved in  
116 bonding (interaction) with oxygen. Similarly Ti is in oxidation state +4 in  $\text{TiO}_2$  as explored in  
117 Figure 1; although, there is again appreciable electron density in the Ti 3d orbitals due to  
118 bond polarisation and weak orbital hybridisation as observed in the electronic density of  
119 states. The next section will explore these ideas in greater depth.

## 120 Determining and Understanding Partial Charges

121 The historical description of chemical interactions, or bonding, involving the sharing and  
122 transfer of integral numbers of electrons was challenged following the development of  
123 quantum mechanics. The distribution of electrons in chemical systems is described by the  
124 many-electron Dirac equation; however, practical treatments require simplification<sup>20</sup>.  
125 Techniques employing one-electron wavefunctions are ubiquitous in quantum chemistry,  
126 and for solids these take the form of periodic (Bloch) functions. By their nature, these  
127 functions are delocalised in real space and cannot be easily interpreted in terms of  
128 individual chemical interactions (covalent bonds, lone pairs, etc.).

129 The link to chemical intuition can be recovered by employing one-electron *localised* orbitals  
130 (e.g. obtained with Foster-Boys and Pipek-Mezey schemes in molecules and Wannier  
131 orbitals in solids, as discussed further below)<sup>21</sup>. However, the complexity of chemical  
132 bonding in many compounds necessities going beyond a one-electron picture, e.g. in the  
133 chemistry of radicals with multi-centre multi-electron interactions. More generally,  
134 electrons can be separated into groups, with strong correlation within a single group, and  
135 weak correlation between them<sup>22,23</sup>.

136 Both experiment and electronic structure based computational techniques are widely used  
137 to obtain electron density maps in solids, with a variety of procedures used to interpret  
138 them in terms of atomic charges. However, individual atomic charges in a multi-electron

139 compound are not a quantum mechanical observable and there is a high degree of  
140 ambiguity both in their definition and in the approaches to calculating them<sup>6</sup>, in contrast to  
141 the simpler and heuristic oxidation state. Nevertheless the concept of partial (atomic)  
142 charges is a useful one and we consider briefly the ways in which it has been formulated and  
143 applied.

144 Determining the electronic density associated with a particular atom or ion in a solid-state  
145 material is in some ways a natural choice to calculate the atomic charges. Indeed,  
146 experimental techniques such as X-ray diffraction (XRD) allow one to measure such  
147 densities, and visualise them in real space via a Fourier transform. Information obtained  
148 from local surface probes including scanning tunnelling microscopy (STM) and atomic force  
149 microscopy (AFM), while limited, can also be used to reconstruct charge density  
150 distributions. At the same time, theoretical techniques provide increasingly accurate  
151 electron density maps in solids. The crucial question then remains: how are these electronic  
152 densities, which are continuous functions through the unit cell of a crystal, partitioned  
153 amongst the constituent atoms? In the vast majority of cases, there is overlap in density  
154 between atoms, making the partitioning a non-trivial problem.

155 A simple approach is to use geometric partitioning, where the charge within a certain radius  
156 or polyhedron, or, in the analysis of Bader<sup>24</sup>, within a contour of zero density gradient is  
157 computed and associated with an atom. An alternative approach is to construct a set of  
158 Wannier functions to associate electrons with each atom<sup>25</sup>; these are Fourier transforms of  
159 Bloch wavefunctions onto discrete centres<sup>26</sup>. These sets of Wannier functions are then  
160 assigned to ionic cores via their spatial proximity. Unfortunately, such methods only provide  
161 a unique and unambiguous definition of atomic charge when both the orbital overlap and  
162 polarisation due to electrostatic fields is zero. Partial charges of real materials vary with the  
163 method employed and the values are difficult to rationalise in terms of integral electron  
164 transfer. A range of such approaches are illustrated in Figure 2 for the case of CdO.

165 The overlap in electron density between atoms can be accounted for through analysis of the  
166 electronic wavefunctions in terms of localised, atom-centred basis functions. Through a  
167 linear combination of atomic orbitals (LCAO) approach, Mulliken's analysis<sup>27</sup> represented  
168 the atomic charge in terms of populations of atomic orbitals. Each pair of atoms has a gross,  
169 net and overlap population, given in terms of the atomic orbital basis set. Originally the  
170 overlap population was divided equally between the interacting ions, but subsequent  
171 improvements on this method have been applied including those of Christoffersen<sup>28</sup>  
172 employing molecular orbitals and Hirshfeld<sup>29</sup> using the charge density, which take into  
173 account to some degree the polarity of the bond between the atoms. Wavefunction-derived  
174 properties, such as the single and pair electron densities have been incorporated in the  
175 electron localisation function (ELF, see Figure 2c)<sup>30</sup>, which describes the probability of  
176 finding an electron close to another in the same spin state and allows one to determine  
177 regions where electrons are localised close to atomic centres<sup>31</sup>. Electronic wavefunction  
178 analysis, however useful, cannot solve the fundamental problem that atomic charge in  
179 compounds is not an observable. Results from such analyses vary strongly with the choice of  
180 basis function and with the method used to determine interactions between atoms,  
181 whether through LCAO parameterised tight-binding methods or *ab initio* techniques.

182 A crucial consideration when modelling atomic charge is the polarisability of the ion in  
183 question. When an electric field is applied to a material, the ions respond not just by  
184 changing their centre of mass coordinates, but also by deformation of their electron clouds.  
185 Displacement upon ionic polarisation can be accounted for in a simple manner, to describe

186 the response to applied electric fields, by attributing an effective charge to the ion. Good  
187 agreement with experimental measurements that probe the dielectric response of a  
188 material can be achieved with this approach<sup>5</sup>. Care must be taken with such effective  
189 charges including the frequently-used Born charge, however, as their derivation, while  
190 useful when modelling the dielectric response of a material, can often mask the underlying  
191 physics. For example, such charges can be used in a rigid-ion model of a crystal to calculate  
192 the vibrational (phonon) modes, but in doing so one is explicitly assuming that the ions are  
193 non-deformable, which greatly limits the transferability of these models. Moreover, the  
194 cohesive energy of a crystal is much less dependent on the polarisability of the constituent  
195 ions than are the lattice vibrational properties. The ionic charge that reproduces cohesive  
196 energies will generally be different from the effective charge that reproduces vibrational  
197 frequencies accurately. This problem can be overcome by using polarisable ions in materials  
198 modelling, e.g. described with the shell model<sup>32</sup>.

199 Taking into account the electronic polarisability of an ion in a solid can remove some of the  
200 ambiguities with regard to defining atomic charges. Indeed, this outcome is expected, given  
201 that the link between polarisability and experimentally observable quantities is far clearer  
202 than that between the poorly defined atomic charges and experiment. In a dielectric crystal,  
203 the dipole moment within a unit cell cannot be uniquely defined owing to the arbitrary  
204 choice in the definition of the unit cell as a result of translation symmetry. However,  
205 differences in polarisation between displaced (atomic and electronic) configurations, which  
206 are the source of experimentally observable quantities, do not depend on the unit-cell  
207 choice. The computation of such differences in polarisation is the aim of the 'modern theory  
208 of polarisation'<sup>27</sup>, in which the electron clouds associated with ions are represented by  
209 Wannier functions. The polarisation difference is usually calculated through topological  
210 analysis of the electron distribution via the Berry phase formalism, from which the number  
211 of Wannier centres (i.e. electrons) that move with a particular atomic displacement can be  
212 derived<sup>33,34</sup>. Thus a partitioning of electrons is achieved, which is not based on spatial  
213 considerations with respect to ion core coordinates, but on the lattice dynamic distribution  
214 of the electronic states. Employing this theory, Jiang et al.<sup>35</sup> obtained ionic partial charges  
215 from first-principles calculations that recovered formal oxidation states for each species in a  
216 diverse set of systems (LiH, water, BaBiO<sub>3</sub> and Sr<sub>2</sub>FeWO<sub>6</sub>). This approach highlights the link  
217 between changes in polarisation and oxidation states that is intuitively satisfying;  
218 nevertheless, it remains one amongst several approaches.

219 Experimental techniques that measure electron density suffer from the same ambiguity as  
220 electronic structure calculations in partitioning to atomic centres. Alternative techniques  
221 can be used to probe atomic charges, beyond those based on measuring the dielectric  
222 response of a material already mentioned. In electrochemical processes, ionic charges are  
223 exchanged in integer numbers through redox reactions. X-ray photoemission spectroscopy  
224 (XPS) is widely used to infer oxidation states via the shifts and splittings of core levels that  
225 act as spectral fingerprints. Another probe is the absorption edge in X-ray Absorption Near  
226 Edge Structure (XANES) measurements, which increases in energy as the oxidation state of  
227 the absorption site increases. Neutron spectroscopy, spin resonance techniques, and other  
228 spectroscopic or magnetic measurements can be used to probe unpaired spin densities,  
229 which can give information on bonding character and from which details on oxidation states  
230 can be inferred<sup>19</sup>.

231 It is useful at this point to draw together the threads of our argument. The concept of  
232 oxidation state is a simple but powerful one. It relates to electron count and indicates the

233 number of electrons from component atoms that are involved in chemical bonding. Charge  
234 density is a distinctive entity, which is accessible from experiment and theory, but whose  
235 partition into atomic charges is intrinsically ambiguous. Provided this crucial factor is  
236 recognised, it is nevertheless a very useful concept and recent approaches to assigning  
237 partial charges tend to align them with oxidation states. Our discussion continues with  
238 examples of systems and problems that pose particular challenges to the twin concepts of  
239 atomic charge and oxidation state.

#### 240 Challenges for Mixed-Valence and Correlated Systems

241 The ongoing debate on oxidation states in more complex or complicated systems keeps the  
242 field open for further refinement. Oxidation states are straightforward to assign in systems  
243 where atoms display a single oxidation state, but they can start to blur in polyion and mixed-  
244 valence compounds, where elements are present in more than one distinct state. Imagine a  
245 system where metal M exists in oxidation states (A and B), occupying two detectable sites in  
246 the crystal (labelled X and Y). The degree of mixing between these two Heitler-London  
247 configurations  $M_X^A M_Y^B$  and  $M_X^B M_Y^A$  will be controlled by how distinguishable the two  
248 crystallographic sites are<sup>36</sup>. Robin and Day categorised these systems into three classes<sup>37</sup>: (i)  
249 Class 1, where the sites are very different and the electrons are completely trapped, (ii)  
250 Class 3, where the sites are indistinguishable and the system has a genuine non-integral  
251 oxidation state, and (iii) Class 2, where the sites are distinguishable, however, not very  
252 different, and so a range of intermediate oxidation state behaviours can be observed.

253 Class 1 compounds should be the easiest to understand; however, the assignment in some  
254 systems still promotes debate. Silver monoxide, (AgO or Ag<sub>2</sub>O<sub>2</sub>) is one such example, where  
255 Ag exists in the +1 and +3 oxidation states, with Ag(I) in a linear coordination between two  
256 oxygen, and Ag(III) in a distorted square planar coordination. Despite these different  
257 crystallographic sites, assignment of the oxidation states present in AgO has been  
258 contentious, with some studies favouring an explanation of Ag(I),Ag(II) with localised hole  
259 polarons on oxygen. This controversy was solved using electronic structure calculations in  
260 tandem with X-ray photoemission and fine-structure analysis<sup>38</sup>. Another Class 1 system,  
261 covelite (CuS) is a mineral in which Cu is found in two distinct coordination environments  
262 (trigonal planar and tetrahedral) and S is also found in different environments, with one  
263 third of the S in a trigonal pyramidal coordination and two thirds present in S—S dimers.  
264 Counter to chemical intuition, the oxidation state of Cu in CuS is thought to be Cu(I) due to  
265 the presence of the S<sub>2</sub><sup>2-</sup> dimers; although, debate remains as to whether there is a mixture of  
266 oxidation states on the Cu sites, on the S sites or on both<sup>39</sup>.

267 Temperature can conspire to make the analysis of oxidation states in mixed valence systems  
268 difficult. At room temperature, magnetite (Fe<sub>3</sub>O<sub>4</sub>) crystallises in a cubic AB<sub>2</sub>O<sub>4</sub> spinel  
269 structure, in which Fe(III) ions occupy the tetrahedral A sites, and a 50:50 ratio of Fe(II) and  
270 Fe(III) ions occupy the octahedral B sites, which can be difficult to distinguish. Below 125 K,  
271 the system undergoes what is known as the Verwey transition, a structural distortion to a  
272 monoclinic superstructure, and becomes electrically insulating, with the charge ordering of  
273 the similarly-sized +2 and +3 ions contentious for many years. Recently, an investigation by  
274 Attfield and co-workers revealed the presence of localised electrons which are distributed  
275 over three linear Fe-site units, termed trimerons<sup>40</sup>. This breakthrough was enabled by large  
276 40-micrometre grains of the low temperature structure, which allowed the identification of  
277 the emergent order.

278 Similarly, pressure can change the nature of charge distributions in a solid, making the  
279 analysis of oxidation states quite complex. Boron is a metalloid that exists in several well-  
280 known allotropes. In nearly all of these allotropes, the structures are made up of icosahedral  
281  $B_{12}$  clusters that feature metallic-like three-centre bonds within each icosahedron, and  
282 covalent two- or three- centre bonds between the icosahedra, satisfying the octet rule and  
283 yielding insulating electronic structures. Under pressures exceeding 19 GPa and less than 89  
284 GPa, boron adopts a novel ionic structure, consisting of an NaCl-type arrangement of  
285 icosahedral  $B_{12}$  clusters and  $B_2$  pairs<sup>41</sup>. The resultant structure is a “boron boride”, perhaps  
286 best characterised by the formula  $(B_2)^{\delta+}(B_{12})^{\delta-}$ .

287 Highly-correlated systems can also present a challenge to our understanding of oxidation  
288 states. Plutonium – important as a nuclear fuel – is situated amongst the actinides in the  
289 periodic table. In the early actinides (Th to Np), the 5f electrons are delocalised, which  
290 allows them to take part in bonding within the lattice, similar to the behaviour of the 5d  
291 series. For the heavier actinides (above Am), the 5f electrons are localized, and do not take  
292 part in bonding. Plutonium is at the cusp of these two behaviours, resulting in one of the  
293 most complex electronic structures for an elemental metal<sup>42</sup>. The ground state has only  
294 recently been conclusively revealed to be a quantum mechanical admixture of localised and  
295 itinerant electronic configurations, with the charge fluctuating between distinct Pu(IV) ( $5f^4$ ),  
296 Pu(III) ( $5f^5$ ) and Pu(II) ( $5f^6$ ) electronic configurations<sup>43</sup>.

297 The breakdown of simple concepts of oxidation state has also been emerging as a key  
298 ingredient in many observations of unconventional critical phenomena, which do not follow  
299 standard spin-fluctuation theories. The quantum criticality of Yb-valence fluctuations have  
300 been shown to be the origin of divergent spin behaviours in  $YbRh_2Si_2$  and  $\beta$ - $YbAlB_4$ ,  $YbAgCu_4$ ,  
301 and  $YbIr_2Zn_{20}$ ,<sup>44</sup> and similarly the valence fluctuations of Ce in  $CeIrIn_5$ .<sup>45</sup> In superconductivity,  
302 nearly critical valence fluctuations has been reported to mediate Cooper pairing in  $CeCu_2Ge_2$   
303 and  $CeCu_2Si_2$  under high pressure<sup>46</sup>.

304 These are examples of challenging cases to the oxidation state concept. Situations where  
305 the assignments of oxidation states become ill-defined are usually those associated with  
306 intriguing new physics that tests our very understanding of chemical bonding in solids.

## 307 Outlook

308 With the ever-increasing arsenal of advanced theoretical methods and experimental  
309 techniques available at present, the misunderstandings of (and challenges to) our  
310 understanding of oxidation states are slowly decreasing. The related but distinct concepts of  
311 oxidation state, atomic charge, and ionicity will remain of key importance in understanding  
312 and describing chemical bonding in general, but particularly in solids. While modern  
313 sophisticated methods may uncover challenges to what are inherently simple and intuitive  
314 investigative tools, the concept of oxidation state, which has survived over two centuries of  
315 use in the chemical sciences, will stay at the core of our description of the interaction of  
316 atoms in molecules and solids, provided the distinctions between it, the atomic charge and  
317 ionicity are fully appreciated.

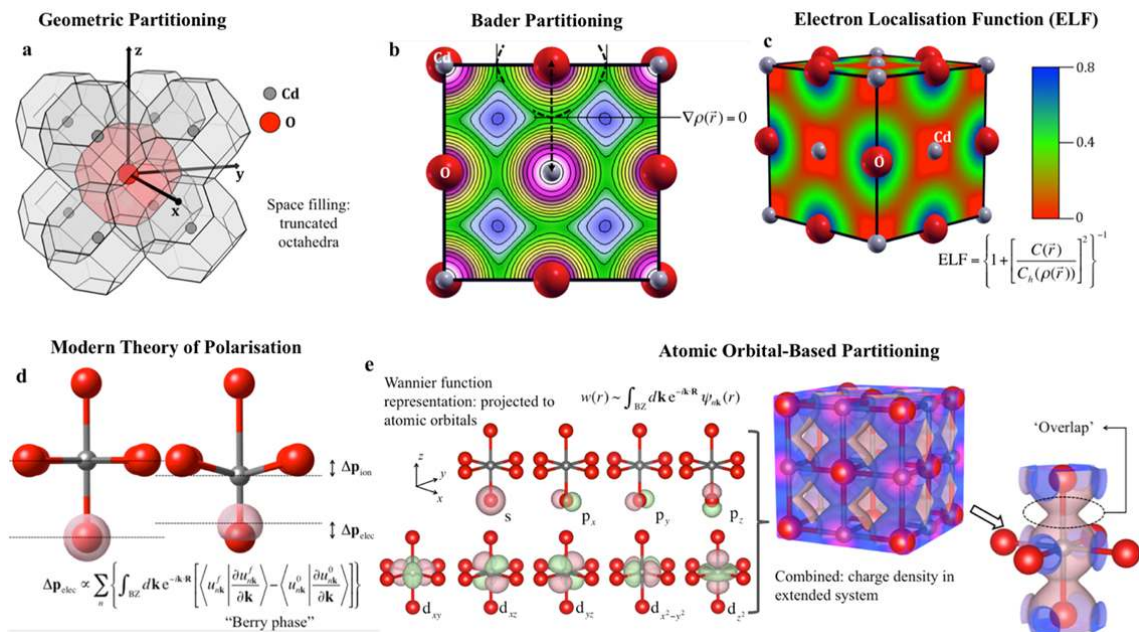
318

319 As our understanding of the structure and properties of diverse materials continues to  
320 improve, we expect a clearer view to emerge of electronic and ionic interactions in highly  
321 challenging systems including new classes of high- $T$  superconductors<sup>47</sup>, boron compounds<sup>48</sup>,  
322 supported metal and semiconductor nanoclusters<sup>49</sup>, layered MXenes<sup>50</sup> and beyond. The key  
323 concepts in electron group theory, the theory of polarisation, supercritical behaviour, and

324 the integral view of microscopic and mesoscopic behaviour of solids including charge and  
325 spin fluctuations are all essential ingredients to the future application and utility of the  
326 oxidation state.  
327  
328







346

347 **Figure 2** Illustration of five approaches for partitioning electron density between atomic  
 348 centres in chemical systems. We use the case of CdO, in which Cd has a formal +2 and O has  
 349 a -2 oxidation state. (a) Geometric partitioning based on space filling for a Wigner-Seitz  
 350 polyhedral decomposition of CdO in a CsCl-like structure. (b) Topological analysis of the  
 351 electron density  $\rho(\vec{r})$  in rocksalt CdO as shown using Bader's Atoms in Molecules approach.  
 352 (c) Analysis of electron pair probability distribution as determined using the electron  
 353 localisation function (ELF – here the functions  $C$  and  $C_h$  are related to the electron pair  
 354 density, see Ref. <sup>30</sup>). (d) Changes in electric polarisation  $\Delta\mathbf{p}$  from topological analysis of the  
 355 electron distribution using the Berry phase formalism applied to standard band structure  
 356 calculations in the Bloch function basis, see Refs. <sup>33,34</sup>. (e) Projection of extended electronic  
 357 wavefunctions onto localised orbitals (Wannier functions,  $w(r)$ , defined again using pre-  
 358 calculated Bloch functions) that combine to reproduce the full electron density of the  
 359 crystal.

360 **Box 1 Assigning formal oxidation states**

361 The oxidation state represents "the degree of oxidation of an atom in terms of counting  
362 electrons" [IUPAC, 2018]. For the simplest cases, the octet (eight electron) rule is sufficient  
363 for electron counting, where atoms are assigned octets in order of decreasing  
364 electronegativity until all valence electrons are distributed. The resulting atom charge then  
365 represents the oxidation state. For example, when Zn ( $3d^{10}4s^2$ ) and O ( $2s^22p^4$ ) are brought  
366 into contact to form ZnO, the octet of O is completed ( $2s^2p^6$ ) with oxidation state -2, while  
367 Zn adopts a  $3d^{10}4s^0$  configuration with oxidation state +2.

368 A set of more general rules for determining oxidation states are provided in undergraduate  
369 chemistry textbooks. For example, following those given in "Inorganic Chemistry" [Mark  
370 Weller, Tina Overton, Jonathan Rourke, and Fraser Armstrong, OUP, 6th Edition, 2014.]:

371 1. The sum of oxidation states for all atoms in the species is zero to ensure electroneutrality

372 2. Atoms in their elemental form: 0

373 3. The available valence electrons follow the Group in the Periodic Table, e.g.

374 Atoms of Group 1: +1

375 Atoms of Group 2: +2

376 Atoms of Group 3: +3

377 Atoms of Group 13: +1 (filled  $s^2$  lone pair) or +3

378 4. Hydrogen in compounds with nonmetals: +1 (hydron)

379 in compounds with metals: -1 (hydride)

380 5. Fluorine: -1

381 6. Oxygen: -2 unless combined with fluorine

382 -1 in peroxides ( $O_2^{2-}$ )

383 -1/2 in superoxides ( $O_2^-$ )

384 -1/3 in ozonides ( $O_3^-$ )

385 7. Halogens: -1 unless other elements include O or more electronegative halogens

386 These rules are sufficient for assigning oxidation states of most solids, but there are caveats  
387 and a number of interesting exceptions are discussed in the main text such as in polyion and  
388 mixed-valence compounds. Many elements, in particular the transition metals, can exist in a  
389 variety of oxidation states.

390 Beyond assignment based on composition alone, as part of crystal structure determination  
391 it is common to use knowledge of the local structure (bond lengths and angles) to assign  
392 oxidation states based on a valence bond analysis<sup>55</sup>. One assignment algorithm involving  
393 analysis of nearest-neighbour coordination environments is implemented in the open-  
394 source PYMATGEN package [<http://pymatgen.org>].

395

396

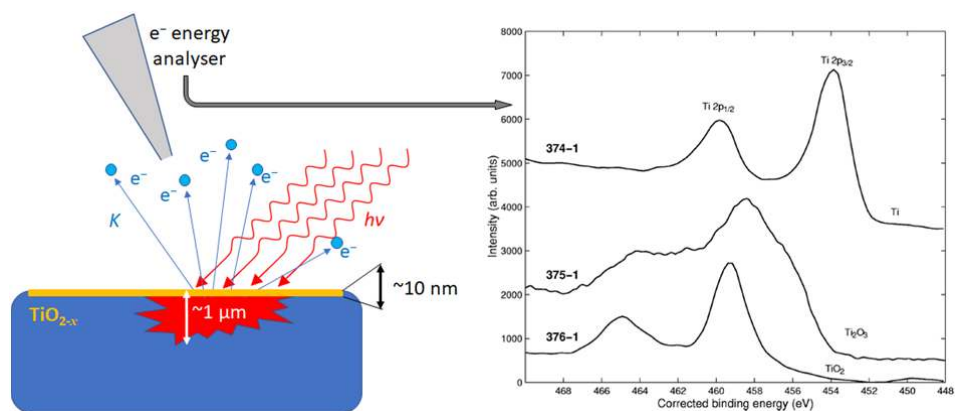
397

398

399 **Box 2 X-ray Photoelectron Spectroscopic (XPS) fingerprints of oxidation states**

400 The experimental technique of X-ray photoelectron spectroscopy (XPS) is a crucial analytical  
401 tool in materials science, which is widely used to assign atomic oxidation states. Based on  
402 the photoelectric effect discovered by H. R. Hertz in 1887 and explained by A. Einstein in  
403 1905, it allows one to probe a range of electronic states in atoms comprising materials or  
404 molecules. The basic process is shown in the schematic below. A source provides a beam of  
405 X-rays of frequency  $\nu$  which impinges on the surface of a sample; electrons are subsequently  
406 excited from bound to empty states in the system and leave the sample under the influence  
407 of an external electric field. By measuring the kinetic energies  $K$  of such photoelectrons, the  
408 binding energies  $E_b$  of the initial states are determined via Einstein's formula:  $E_b = K -$   
409  $h\nu - \Phi$ , where  $\Phi$  is the work function of the sample. The frequency of the X-rays  
410 determines which electronic states are probed and how deep within the sample the  
411 photons can penetrate. It is therefore possible, by varying the frequency, to probe states  
412 varying from the valence band to deep within the atomic core. Moreover, lower frequencies  
413 allow one to analyse surface electronic states (so-called soft XPS), while high frequencies are  
414 used to probe states within the bulk of the sample (hard XPS).

415



416

417

418 The theory of the process developed by K. Siegbahn considers the effect of both the initial  
419 and final state of the excited electron, and relates the quantised bands in the observed  
420 spectroscopic signatures to the "true" electron energies in the material, which are  
421 characteristic of particular elements in particular chemical states. By calibrating the  
422 experimental detectors against known 'reference' samples, one can determine chemical  
423 shifts in certain bands that arise due to changes in the chemical environment. For example,  
424 a change in the oxidation state of Ti between that in its metallic phase to the fully oxidised  
425 form of  $TiO_2$  results in an observed shift of 4.6 eV in its 2p core levels, as shown in the  
426 schematic, where the data are taken from Ref. <sup>56</sup>. The XPS measurements employed to  
427 distinguish chemical elements and their electronic states are often referred to as Electron  
428 Spectroscopy for Chemical Analysis, or ESCA.

429

430 Care should be taken in the experimental setup regarding sample preparation, where  
431 charging effects will influence the observed work function and where surface  
432 inhomogeneity will give rise to specific spectroscopic signatures. As the chemical  
433 environment around atoms of interest will affect both the energy and line shapes, and a  
434 number of electronic terms may coexist even within one oxidation state, curve fitting  
435 procedures are applied to separate individual contributions. Such analysis yields valuable  
436 information about the chemical nature of the material's constituent elements. Moreover,

437 the electronic state of an atom/ion in the material may experience fluctuations, and will do  
438 so necessarily in metals either intrinsically or upon a local photoexcitation during the  
439 measurement. If the time of fluctuation is small, (for example in intra-ionic processes) only  
440 the line shape will change. For long times (characteristic of inter-ionic charge transfer  
441 processes), however, the XPS measurement can resolve different oxidation states and  
442 involved electronic terms.  
443

444 **References**

- 445 1. Karen, P. Oxidation state, a long-standing issue! *Angew. Chemie - Int. Ed.* **54**, 4716–  
446 4726 (2015).
- 447 2. IUPAC gold book. Available at: <https://goldbook.iupac.org/O04365.html>.
- 448 3. Goodman, C. H. L. Ionic-covalent bonding in crystals. *Nature* **187**, 590–591 (1960).
- 449 4. Mooser, E. & Pearson, W. B. The ionic character of chemical bonds. *Nature* **1920**,  
450 406–408 (1961).
- 451 5. Cochran, W. ‘Effective’ ionic charge in crystals. *Nature* **191**, 60–61 (1961).
- 452 6. Catlow, C. R. A. & Stoneham, A. M. Ionicity in solids. *J. Phys. C Solid State* **16**, 4321–  
453 4338 (1983).
- 454 7. Raebiger, H., Lany, S. & Zunger, A. Charge self-regulation upon changing the oxidation  
455 state of transition metals in insulators. *Nature* **453**, 763–766 (2008).
- 456 8. Jansen, M. & Wedig, U. A piece of the picture - misunderstanding of chemical  
457 concepts. *Angew. Chemie - Int. Ed.* **47**, 10026–10029 (2008).
- 458 9. Koch, D. & Manzhos, S. On the charge state of titanium in titanium dioxide. *J. Phys.*  
459 *Chem. Lett.* **8**, 1593–1598 (2017).
- 460 10. Walsh, A., Sokol, A. A., Buckeridge, J., Scanlon, D. O. & Catlow, R. A. Electron counting  
461 in solids: oxidation states, partial charges, and ionicity. *J. Phys. Chem. Lett.* **8**, 2074–  
462 2075 (2017).
- 463 11. Pauling, L. The modern theory of valency. *J. Chem. Soc.* 1461–1467 (1948).
- 464 12. Massidda, S., Yu, J., Freeman, A. J. & Koelling, D. D. Electronic structure and  
465 properties of  $\text{YBa}_2\text{Cu}_3\text{O}_{7-\delta}$ , a low dimensional, low density of states superconductor.  
466 *Phys. Lett. A* **122**, 198–202 (1987).
- 467 13. Kageyama, H. *et al.* Expanding frontiers in materials chemistry and physics with  
468 multiple anions. *Nat. Commun.* **9**, 772 (2018).
- 469 14. Zhang, J. *et al.* Designing high-performance layered thermoelectric materials through  
470 orbital engineering. *Nat. Commun.* **7**, 10892 (2016).
- 471 15. Zeier, W. G. *et al.* Engineering half-Heusler thermoelectric materials using zintl  
472 chemistry. *Nat. Rev. Mater.* **1**, 16032 (2016).
- 473 16. Gillespie, R. J. The valence-shell electron-pair repulsion (vsepr) theory of directed  
474 valency. *J. Chem. Educ.* **40**, 295 (1963).
- 475 17. Griffith, J. & Orgel, L. Ligand-field theory. *Q. Rev.* **11**, 381 (1957).
- 476 18. Cockayne, E., Levin, I., Wu, H. & Llobet, A. Magnetic structure of bixbyite  $\alpha\text{-Mn}_2\text{O}_3$ : a  
477 combined DFT+U and neutron diffraction study. *Phys. Rev. B* **87**, 184413 (2013).
- 478 19. Xiong-Fei Shen, <sup>†</sup> *et al.* A magnetic route to measure the average oxidation state of  
479 mixed-valent manganese in manganese oxide octahedral molecular sieves (OMS).  
480 (2005). doi:10.1021/JA043406A
- 481 20. Dirac, P. A. M. Quantum mechanics of many-electron systems. *Proc. R. Soc. London A*  
482 *Math. Phys. Eng. Sci.* **123**, 714 (1929).
- 483 21. Szabo, A. & Ostlund, N. S. *Modern quantum chemistry : introduction to advanced*  
484 *electronic structure theory*. (Dover Publications, 1996).
- 485 22. Mcweeny, R. The density matrix in many-electron quantum mechanics. i. generalized  
486 product functions. factorization and physical interpretation of the density matrices.  
487 *Proc. R. Soc. Lond. A. Math. Phys. Sci.* **253**, 242–259 (1959).
- 488 23. Kantorovich, L. N. & Zapol, B. P. A diagram technique for nonorthogonal electron  
489 group functions. i. right coset decomposition of symmetric group. *J. Chem. Phys.* **96**,  
490 8420–8426 (1992).
- 491 24. Bader, R. F. W. & Nguyen-Dang, T. T. Quantum theory of atoms in molecules-dalton

- 492 revisited. *Adv. Quantum Chem.* **14**, 63–124 (1981).
- 493 25. Kohn, W. Analytic properties of bloch waves and wannier functions. *Phys. Rev.* **115**,  
494 809–821 (1959).
- 495 26. Marzari, N. & Vanderbilt, D. Maximally localized generalized wannier functions for  
496 composite energy bands. *Phys. Rev. B* **56**, 12847–12865 (1997).
- 497 27. Mulliken, R. S. Electronic population analysis on lcao–mo molecular wave functions. i.  
498 *J. Chem. Phys.* **23**, 1833–1840 (1955).
- 499 28. Christoffersen, R. E. & Baker, K. A. Electron population analysis. gross atomic charges  
500 in molecules. *Chem. Phys. Lett.* **8**, 4–9 (1971).
- 501 29. Hirshfeld, F. L. Bonded-atom fragments for describing molecular charge densities.  
502 *Theor. Chim. Acta* (1977). doi:10.1007/BF00549096
- 503 30. Becke, A. D. & Edgecombe, K. E. A simple measure of electron localization in atomic  
504 and molecular systems. *J. Chem. Phys.* **92**, 5397–5403 (1990).
- 505 31. Savin, A. *et al.* Electron localization in solid-state structures of the elements: the  
506 diamond structure. *Angew. Chemie Int. Ed. English* **31**, 187–188 (1992).
- 507 32. Dick, B. G. & Overhauser, A. W. Theory of the dielectric constants of alkali halide  
508 crystals. *Phys. Rev.* **112**, 90 (1958).
- 509 33. Spaldin, N. A. A beginners guide to the modern theory of polarization. *J. Solid State*  
510 *Chem.* **195**, 2–10 (2012).
- 511 34. King-Smith, R. D. & Vanderbilt, D. Theory of polarization of crystalline solids. *Phys.*  
512 *Rev. B* (1993). doi:10.1103/PhysRevB.47.1651
- 513 35. Jiang, L., Levchenko, S. V. & Rappe, A. M. Rigorous definition of oxidation states of  
514 ions in solids. *Phys. Rev. Lett.* **108**, 166403 (2012).
- 515 36. Day, P., Hush, N. S. & Clark, R. J. H. Mixed valence: origins and developments. *Philos.*  
516 *Trans. A. Math. Phys. Eng. Sci.* **366**, 5–14 (2008).
- 517 37. Robin, M. B. & Day, P. Mixed valence chemistry—a survey and classification. *Adv.*  
518 *Inorg. Chem. Radiochem.* **10**, 247–422 (1968).
- 519 38. Allen, J. P., Scanlon, D. O. & Watson, G. W. Electronic structure of mixed-valence  
520 silver oxide ago from hybrid density-functional theory. *Phys. Rev. B* **81**, 161103  
521 (2010).
- 522 39. Conejeros, S., Moreira, I. de P. R., Alemany, P. & Canadell, E. Nature of holes,  
523 oxidation states, and hypervalency in covellite (cus). *Inorg. Chem.* **53**, 12402–12406  
524 (2014).
- 525 40. Senn, M. S., Wright, J. P. & Attfield, J. P. Charge order and three-site distortions in the  
526 verwey structure of magnetite. *Nature* **481**, 173–176 (2012).
- 527 41. Oganov, A. R. *et al.* Ionic high-pressure form of elemental boron. *Nature* **457**, 863–  
528 867 (2009).
- 529 42. Albers, R. C. Condensed-matter physics: an expanding view of plutonium. *Nature* **410**,  
530 759–761 (2001).
- 531 43. Janoschek, M. *et al.* The valence-fluctuating ground state of plutonium. *Sci. Adv.* **1**,  
532 e1500188 (2015).
- 533 44. Watanabe, S. & Miyake, K. Quantum valence criticality as an origin of unconventional  
534 critical phenomena. *Phys. Rev. Lett.* **105**, 186403 (2010).
- 535 45. Watanabe, S. & Miyake, K. Roles of critical valence fluctuations in ce- and yb-based  
536 heavy fermion metals. *J. Phys. Condens. Matter* **23**, 094217 (2011).
- 537 46. Yamaoka, H. *et al.* Role of valence fluctuations in the superconductivity of ce122  
538 compounds. *Phys. Rev. Lett.* **113**, 086403 (2014).
- 539 47. Putzke, C. *et al.* Anomalous critical fields in quantum critical superconductors. *Nat.*

- 540 *Commun.* **5**, 5679 (2014).
- 541 48. Mondal, S. *et al.* Experimental evidence of orbital order in  $\alpha$ - $\beta$  and  $\gamma$ - $\beta$  28  
542 polymorphs of elemental boron. *Phys. Rev. B* **88**, 024118 (2013).
- 543 49. Nilsson Pingel, T., Jørgensen, M., Yankovich, A. B., Grönbeck, H. & Olsson, E. Influence  
544 of atomic site-specific strain on catalytic activity of supported nanoparticles. *Nat.*  
545 *Commun.* **9**, 2722 (2018).
- 546 50. Anasori, B., Lukatskaya, M. R. & Gogotsi, Y. 2D metal carbides and nitrides (mxenes)  
547 for energy storage. *Nat. Rev. Mater.* **2**, 16098 (2017).
- 548 51. Jiang, B., Zuo, J. M., Jiang, N., O’Keeffe, M. & Spence, J. C. H. Charge density and  
549 chemical bonding in rutile,  $\text{TiO}_2$ . *Acta Crystallogr. Sect. A Found. Crystallogr.* **59**, 341–  
550 350 (2003).
- 551 52. Scanlon, D. O. *et al.* Band alignment of rutile and anatase  $\text{TiO}_2$ . *Nat. Mater.* **12**, 798–  
552 801 (2013).
- 553 53. Burdett, J. K. Structural–electronic relationships in rutile. *Acta Crystallogr. Sect. B* **51**,  
554 547–558 (1995).
- 555 54. Morgan, B. J. & Watson, G. W. A density functional theory + *u* study of oxygen  
556 vacancy formation at the (110), (100), (101), and (001) surfaces of rutile  $\text{TiO}_2$ . *J. Phys.*  
557 *Chem. C* **113**, 7322–7328 (2009).
- 558 55. Brown, I. D. (Ian D. *The chemical bond in inorganic chemistry : the bond valence*  
559 *model*. (Oxford University Press, 2002).
- 560 56. Kurtz, R. L. & Henrich, V. E. Comparison of Ti 2p core-level peaks from  $\text{TiO}_2$ ,  $\text{Ti}_2\text{O}_3$ , and  
561 Ti metal, by xps. *Surf. Sci. Spectra* **5**, 179 (1998).
- 562

563 **Correspondence and requests for materials should be addressed to** A. W.

564 ([a.walsh@imperial.ac.uk](mailto:a.walsh@imperial.ac.uk)) or C. R. A. C. ([c.r.a.catlow@ucl.ac.uk](mailto:c.r.a.catlow@ucl.ac.uk)).

565

566 **Acknowledgements** This work was supported by the EPSRC (grant nos. EP/K016288/1 and  
567 EP/N01572X/1), the Leverhulme Trust, and the Royal Society. DOS acknowledges support  
568 from the European Research Council (grant no. 758345). This work was carried out with  
569 funding from the Faraday Institution ([faraday.ac.uk](http://faraday.ac.uk); EP/S003053/1), grant number FIRG003.

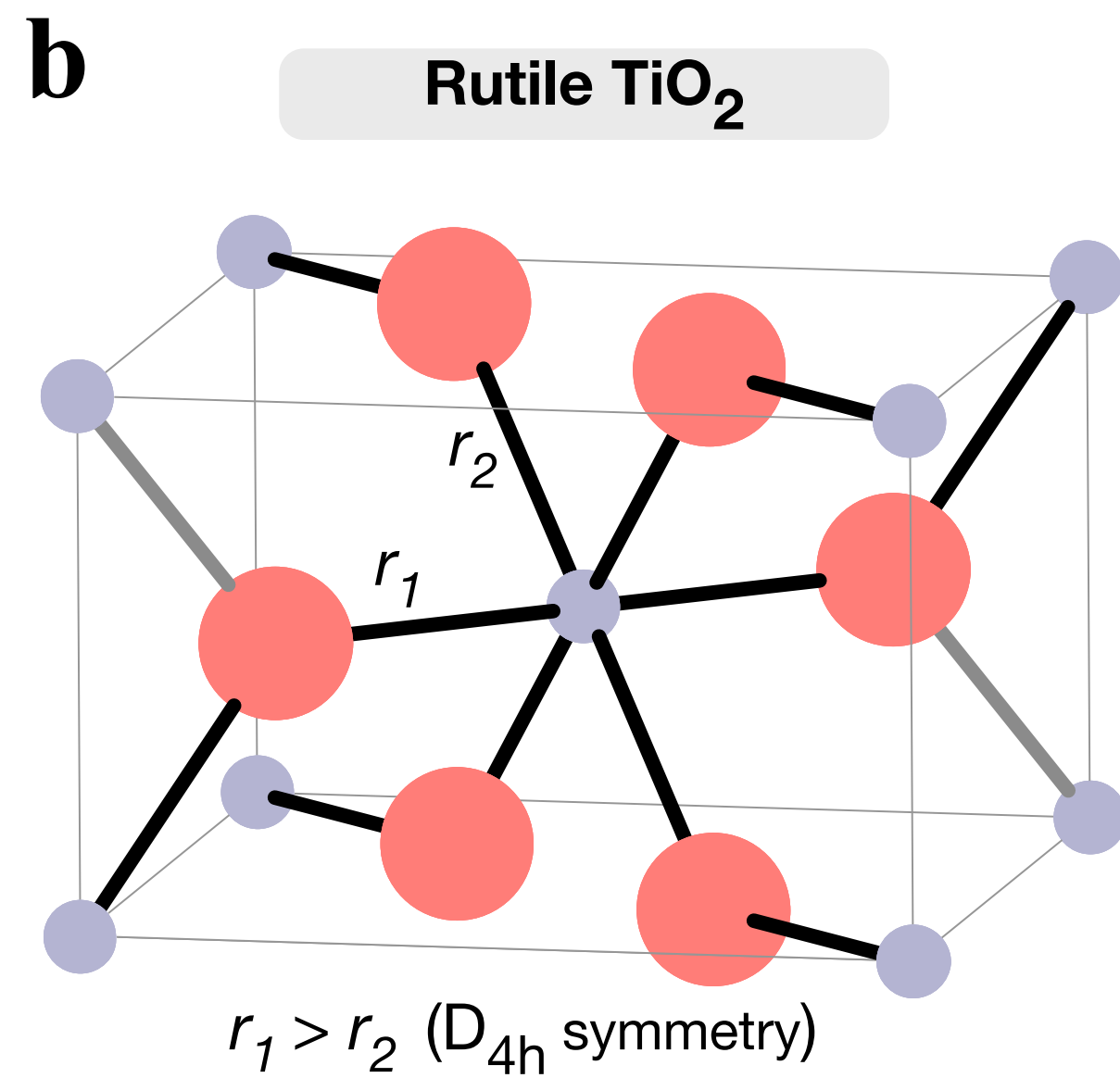
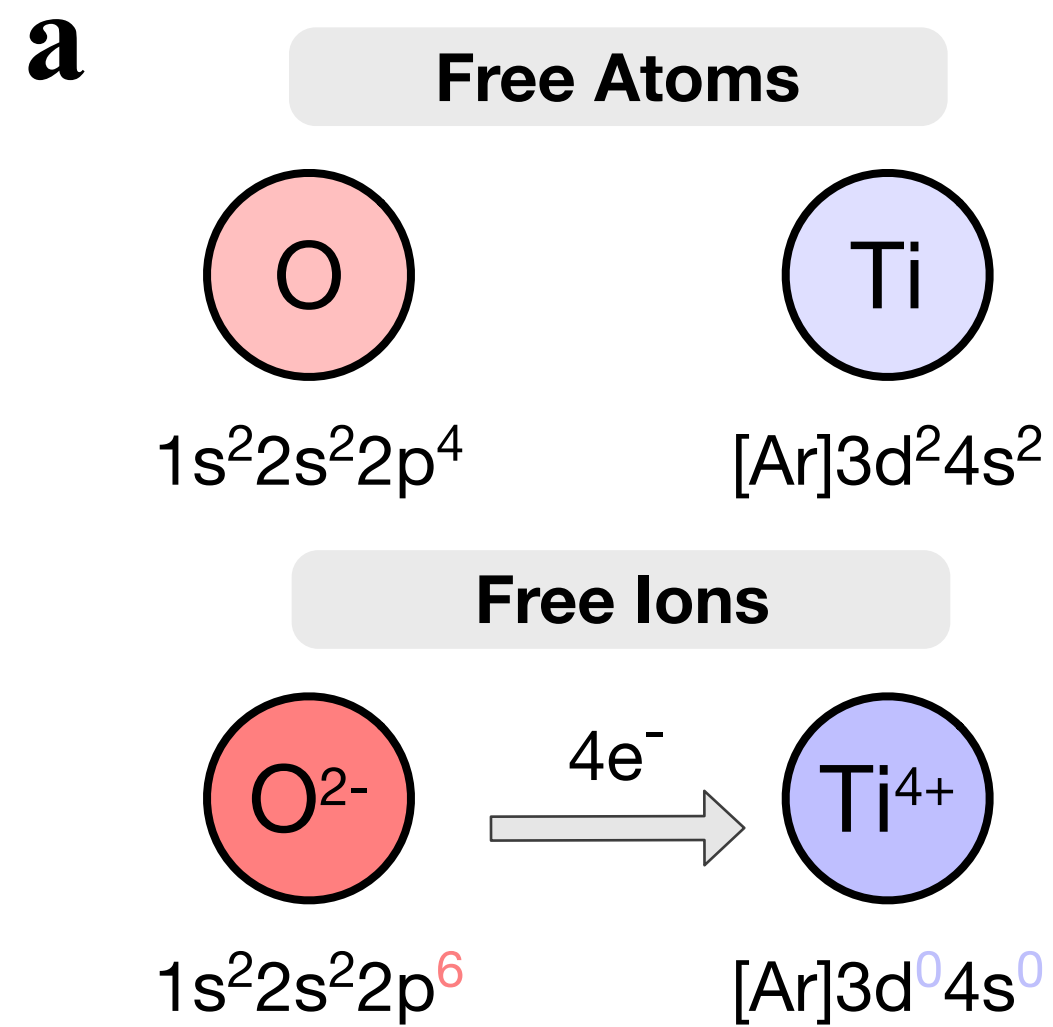
570

571 **Author contributions** All authors contributed equally to the design, writing and editing of  
572 the manuscript.

573

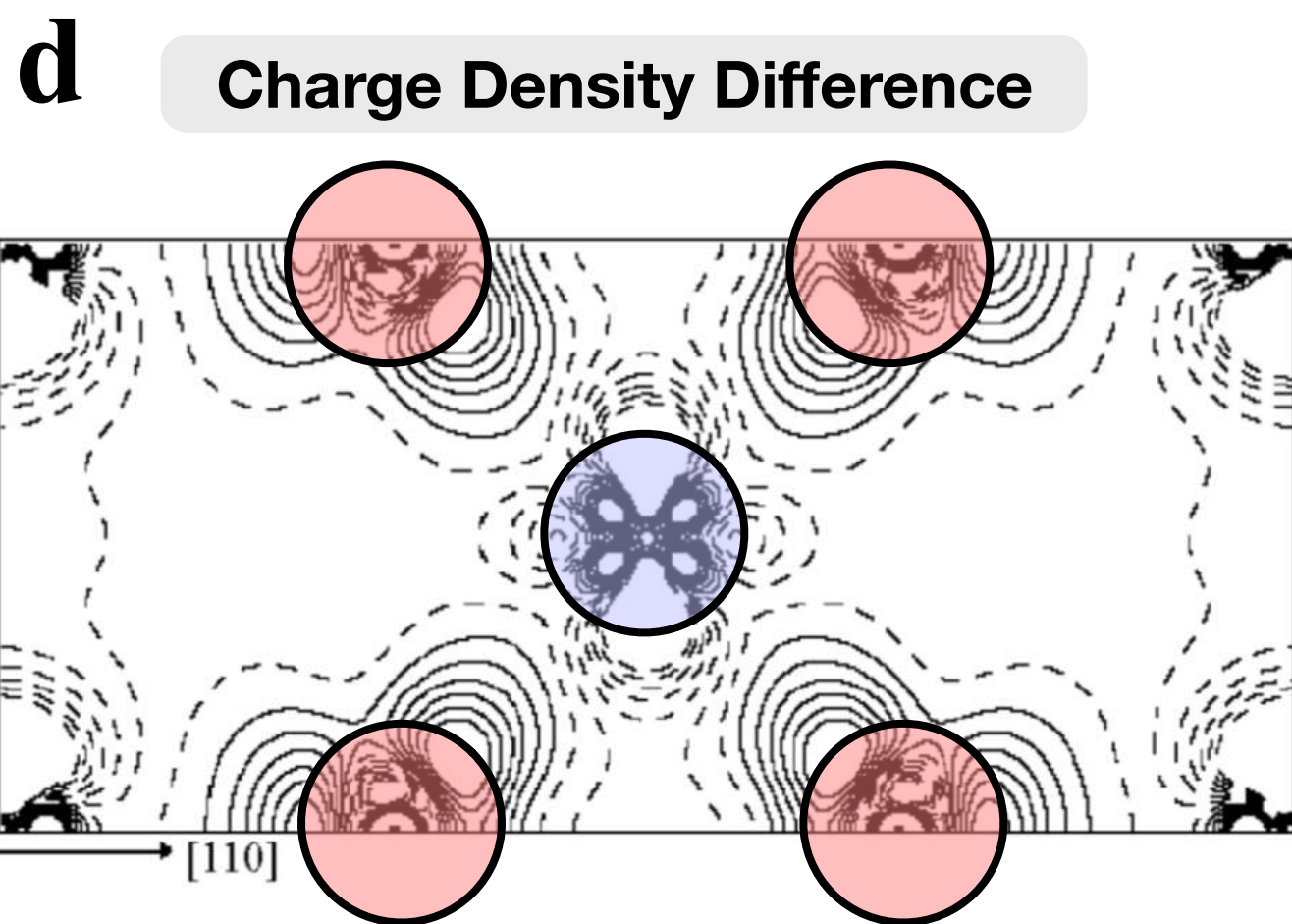
574 **Competing interests** The authors declare no competing interests.



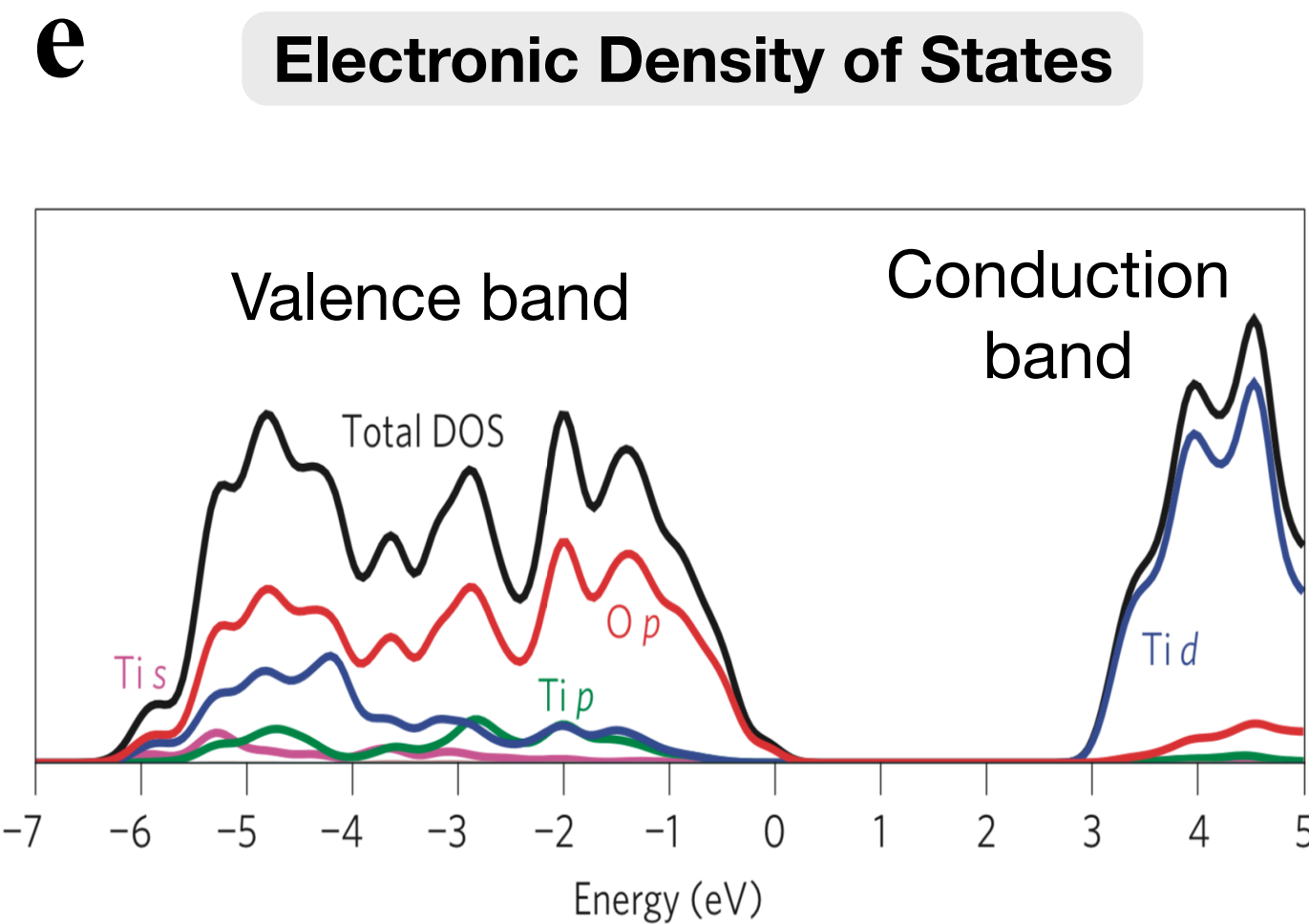


**c** **Probes of Charge Distribution**

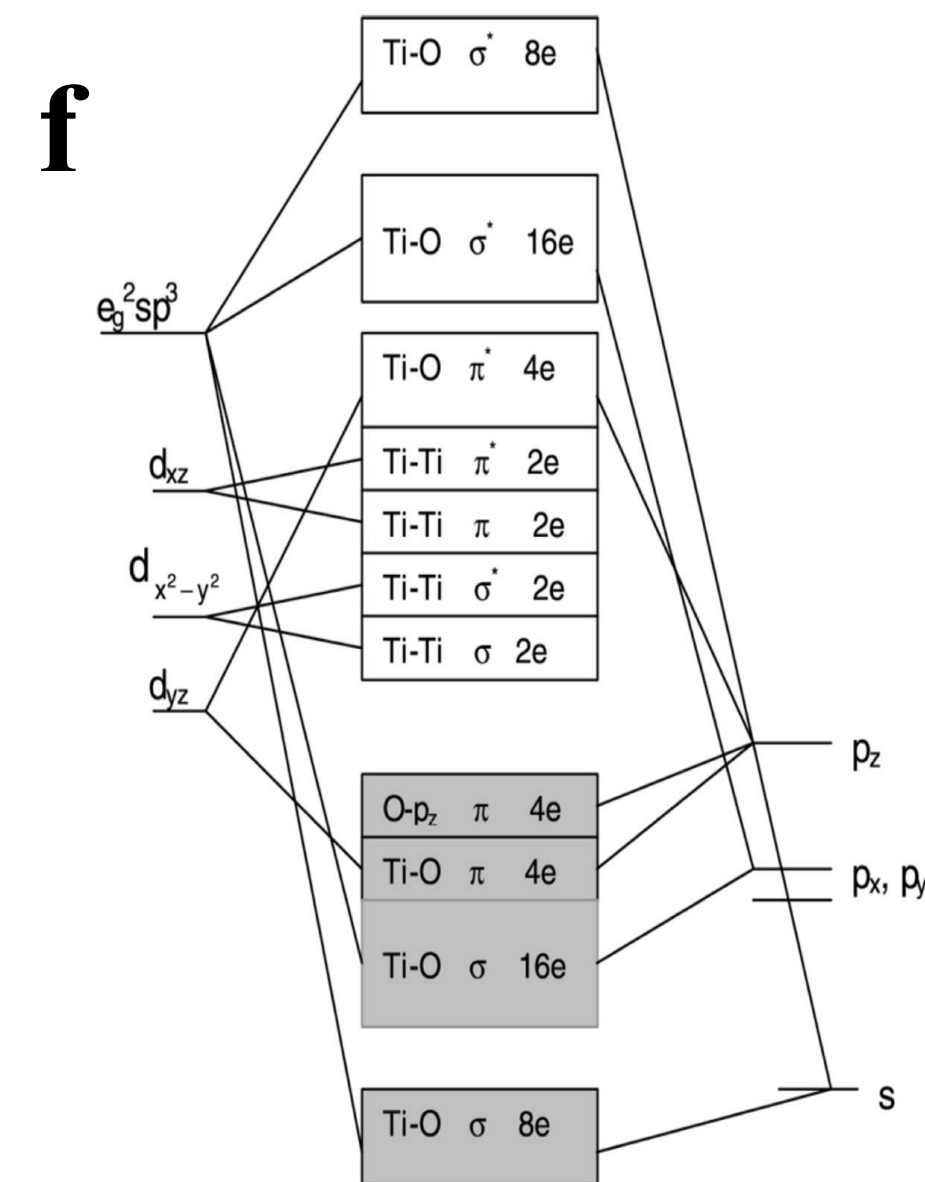
- Structural**: Consistent with  $d^0$  Ti: no Jahn-Teller distortion
- Vibrational**: Large  $\omega_{LO} / \omega_{TO}$  splitting:  $E_u = 494 / 842 \text{ cm}^{-1}$
- Electronic**: X-ray photoemission: O 2p upper valence band
- Dielectric**: Born effective charge tensor of Ti: +5 to +7
- Magnetic**: Diamagnetic Ti(IV); paramagnetic Ti(III) on reduction
- Optical**: Transparent crystal: 3.2 eV excitation from O to Ti
- Chemical**: No further oxidation from  $TiO_2$



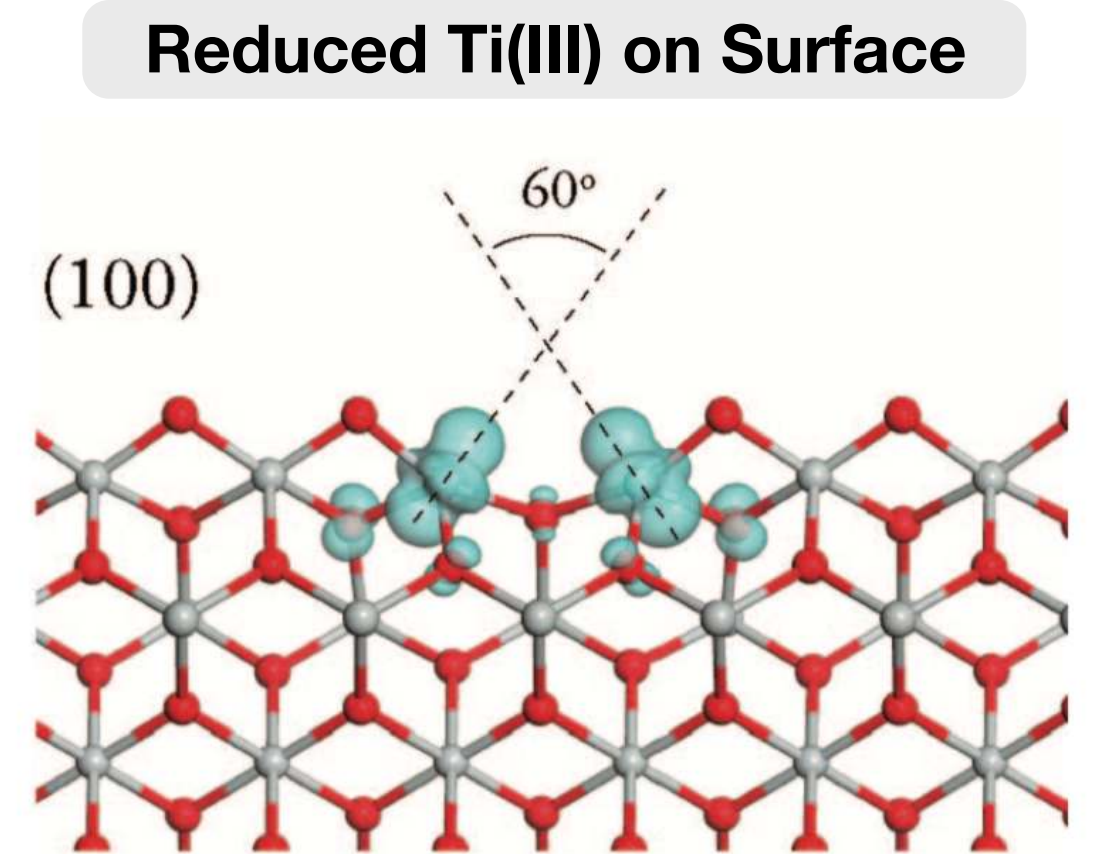
Combined from X-ray and electron diffraction with respect to neutral atoms



Density functional theory calculations confirms Ti 3d conduction band

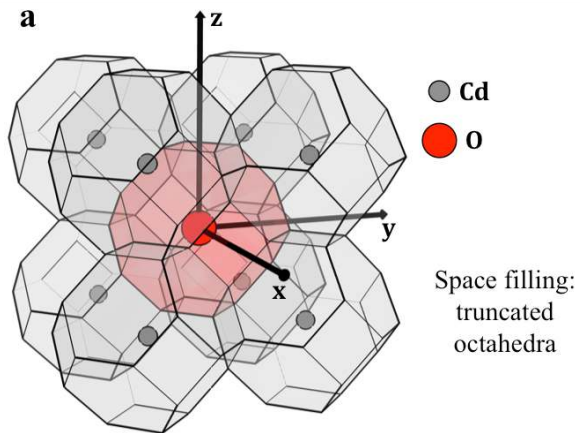


Molecular orbital scheme describing hybridisation between O (left) and Ti (right)

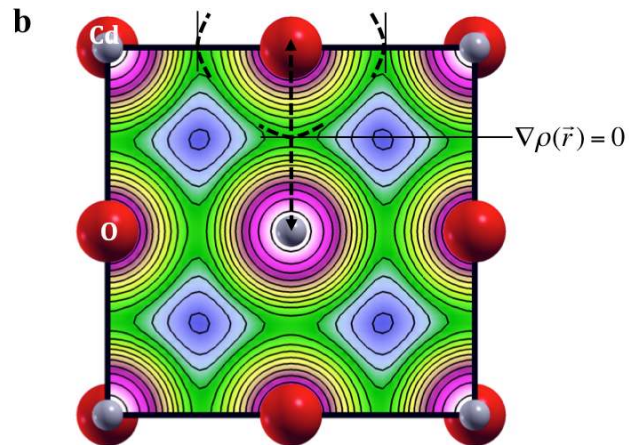


Oxygen vacancy generates two Ti(III)  $d^1$  centres

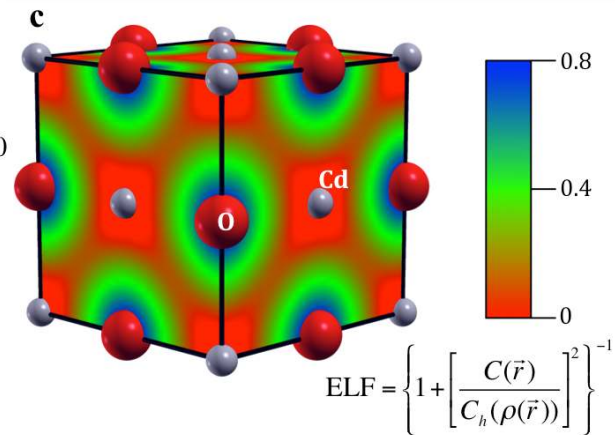
## Geometric Partitioning



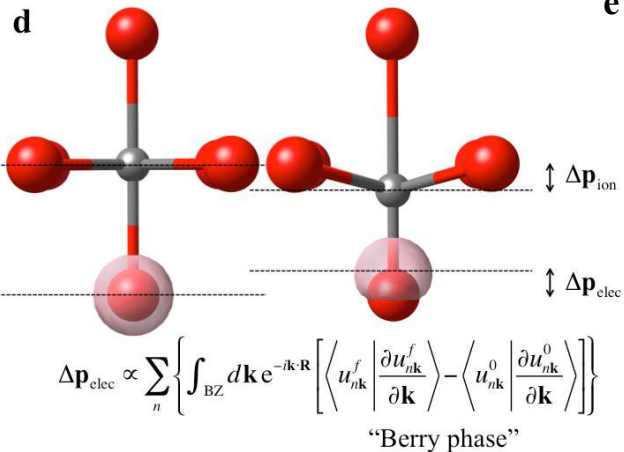
## Bader Partitioning



## Electron Localisation Function (ELF)



## Modern Theory of Polarisation



## Atomic Orbital-Based Partitioning

